

Modeling hybridization kinetics

Jian-Ying Wang ^{*}, Karl Drlica

The Public Health Research Institute, 225 Warren Street, Newark, NJ 07103, USA

Received 17 July 2002; accepted 15 November 2002

Abstract

Formation of complementary base pairs between nucleic acids over a short region (≤ 15 nucleotides) is described by a kinetic model in which the intermediate state is assumed to be locally single stranded. The model enables calculation of a rate factor that is proportional to the rate constant for hybridization under steady-state reaction conditions. Rate factors calculated for various sites in acetylcholinesterase mRNA correlated with sites found previously to be experimentally accessible for hybridization to antisense oligonucleotides. Hybridization rate of longer antisense oligodeoxynucleotides was modeled by calculation of a maximal rate factor for all possible 15-nucleotide segments of a given antisense molecule. Maximal rate factor calculated for a set of antisense oligonucleotides correlated ($r = 0.95$) with initial rate of hybridization reported previously. Two other models proposed for identifying accessible sites for hybridization were less predictive than the rate factor calculation.

© 2003 Elsevier Science Inc. All rights reserved.

Keywords: Antisense; Site selection; Hybridization kinetics; Inhibition; Hybridization rate; Hybridization thermodynamics; RNA target accessibility

1. Introduction

DNA–RNA and RNA–RNA hybridization are important to many aspects of nucleic acid function including DNA replication, transcription, and translation. Hybridization is also central to a variety of technologies that either detect a particular nucleic acid or alter its expression. Hybridization can be characterized with two parameters: equilibrium yield and annealing rate. Equilibrium yield is the main concern when incubation time is unlimited. Such is the case with Southern hybridization. When hybridization is involved in the inhibition of gene expression inside

^{*} Corresponding author. Tel.: +1-973 854 3361.

E-mail address: jian@phri.org (J.-Y. Wang).

cells, hybridization rate is probably more important. For example, in exponentially growing cells, metabolism of cellular RNAs is at steady state. Under these conditions, RNAs are constantly generated and degraded even though their concentrations are constant. In this situation antisense agents must anneal to the target rapidly to be effective [1].

Previous efforts at computational identification of effective antisense oligonucleotides for hybridization to target RNA fall into two categories. In one, predictions of RNA secondary structure are used to identify regions likely to be single stranded and presumably accessible for hybridization [2–6]. Correlation with antisense oligodeoxynucleotide (ODN) hybridization shows considerable scatter, and we now know that single-stranded regions, identified by nucleases, do not correspond to regions that hybridize most readily (see Fig. 3 in Ref. [7]). In a second approach, overall energy gain due to hybrid formation is calculated and related to inhibition of gene expression [8–10]. Sometimes overall energy gain correlates with experimental data, and sometimes it does not [8,9]. More problematic is the inability of energy gain calculations to explain the large (up to 1000 fold) difference in hybridization rate that can exist among different sites [11]. These general problems with existing computational models have made it necessary to use experimental methods to determine favorable sites for antisense attack of RNA. Such methods generally involve hybridization of oligonucleotide libraries to target RNA [7,11–14].

In the present work we raise the possibility that both melting energy and energy gain are important factors in determining accessibility for hybridization. To test the idea, we developed a computational description for hybridization of short complementary regions within large nucleic acids that relates the overall steady-state rate constant to both the melting energy that must be overcome to form a hybrid and to the free energy that is gained as a result of hybrid formation. The resulting relationship makes it possible to calculate a rate factor that is proportional to the rate at which oligonucleotides hybridize to sites in RNA under quasi steady-state conditions (not to be confused with equilibrium or stationary growth conditions). RNA secondary structure, which is expected to impede binding of oligonucleotides to long RNA targets [15], is taken into account by using commercially available RNA structure algorithms to calculate melting energy and energy difference (energy gain). We calculated rate factors for hybridization of ODNs complementary to two RNA species and compared the values to accessibility or hybridization rate that had been measured previously by other laboratories. The correlation between rate factor and experimental data, plus a poorer fit between data and models based on either single-stranded regions [4] or energy gain [9], provide support for the rate factor model.

2. Results

2.1. Theoretical considerations

The hybridization of a short antisense nucleic acid to an RNA target or formation of an initial base-pairing contact between short regions of two large complementary nucleic acids, followed by the subsequent destruction of the target or a conformational change of the target, can be described by



where A is an antisense oligonucleotide, S is the target RNA, AS is the antisense–target RNA hybrid, P represents the products of the second step, k_1 and k_{-1} are the rate constants for binding and dissociation, respectively, and k_2 is the rate constant of the second step, which is assumed to be irreversible. The second step may be an enzymatic cleavage, as in the case of antisense DNA-mediated RNase H cleavage reactions, or it may be a structural change, as in the case of annealing of long antisense–target RNA hybridization.

We modeled hybridization rate in a way similar to that commonly used to calculate chemical reaction rates [16]. In the model, the activated state is considered to be an intermediate in which structures within the region that will hybridize are melted (Fig. 1; for purpose of calculation the intermediates are considered before alignment in the transition state). Three parameters are relevant to the kinetics of hybridization: the melting energy, ΔG_m (the energy increase required to melt the structures in the target site and in the antisense), the hybridization energy, ΔG_h (the energy decrease upon formation of a hybrid between the melted antisense oligonucleotide and the melted target site), and the energy difference or energy advantage, ΔG_d , between the final and the initial states. From these considerations we derived an expression that relates the target disappearance rate constant at steady state to the melting energy and the energy difference.

We begin the derivation with the rate of hybrid concentration change for reactions described by reaction 1. By considering the incoming flow, $k_1[A][S]$, and outgoing flow, $k_{-1}[AS]$ and $k_2[AS]$, we have

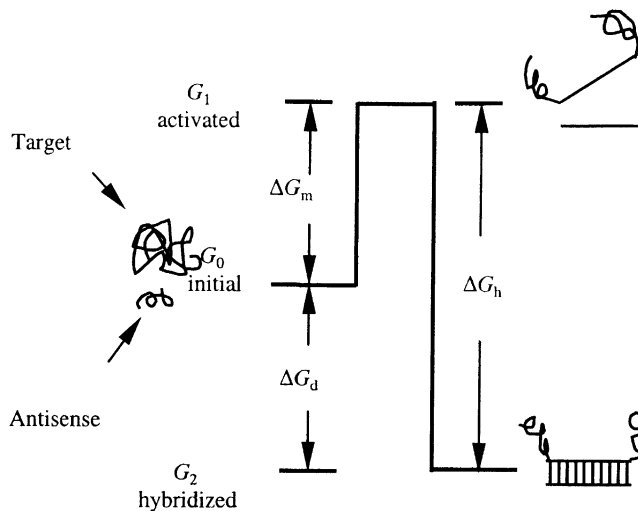


Fig. 1. Energetics of hybridization between antisense and target RNA. Before hybridization can occur, target and antisense (initial free energy = G_0) must become single stranded in the region of interaction (activated free energy = G_1). The free energy required for melting the structure of the hybridization region is termed melting energy ($\Delta G_m = G_1 - G_0$). Hybridization results in a lower energy state (hybridized free energy = G_2). The free energy difference between the hybridized state and the activated state ($G_2 - G_1$) is represented by ΔG_h . The free energy difference between the state after hybridization and the state prior to hybridization ($G_2 - G_0$) is represented by ΔG_d . In a typical case, ΔG_m is positive and ΔG_h and ΔG_d are negative.

$$d[AS]/dt = k_1[A][S] - k_{-1}[AS] - k_2[AS]. \quad (2)$$

To obtain an explicit expression for the rate of target disappearance relevant to intracellular (steady-state) conditions, we utilized the same kinetic approach for the description of quasi steady-state conditions as used by Briggs and Haldane (see Ref. [17]). In such a situation, the hybrid concentration, $[AS]$, is constant or $d[AS]/dt = 0$; consequently,

$$[AS] = \frac{k_1}{k_{-1} + k_2} [A][S]. \quad (3)$$

The rate of product formation, which is also the target disappearance rate, is described by

$$dP/dt = k_2[AS] = \frac{k_2 k_1}{k_{-1} + k_2} [A][S] = \frac{k_2}{K_m} [A][S], \quad (4)$$

in which

$$K_m = \frac{k_{-1} + k_2}{k_1}. \quad (5)$$

Thus from Eq. (4), the second-order association constant for quasi steady-state conditions is

$$k = k_2/K_m. \quad (6)$$

For the initial rate of a single-tube assay, total antisense is conserved. Consequently, the initial antisense concentration, $[A_0]$, equals $[A] + [AS]$ (at the beginning, $[P] \sim 0$). Substitution for $[A]$ in Eq. (2) with $([A_0] - [AS])$ leads to

$$dP/dt = k_2[AS] = \frac{k_2[A_0][S]}{K_m + [S]}, \quad (7)$$

for which the second order association constant is

$$k = \frac{k_2}{K_m + [S]}. \quad (8)$$

Estimation of K_m using Eqs. (6) and (8) enables us to compare relative reaction rates for different sites in a given RNA if k_2 is approximately constant. To estimate K_m first consider k_{-1}/k_1 . Since this ratio is the equilibrium constant for hybrid dissociation,

$$k_{-1}/k_1 = e^{\Delta G_d/RT}. \quad (9)$$

Next consider k_1 , which for long targets is determined by the melting energy barrier that impedes hybridization. From the Boltzmann distribution, the occupancy of the activated state is proportional to $e^{-\Delta G_m/RT}$. Following Pauling [16],

$$k = k_1^* e^{-\Delta G_m/RT}, \quad (10)$$

where k_1^* is the forward rate constant for the binding of the activated (melted) antisense oligonucleotide to the activated (melted) target site. Although k_1^* is related to assay conditions, including cation concentration and temperature, it is independent of RNA structure (the effect of structure is described by $e^{-\Delta G_m/RT}$ in Eq. (10)). Thus k_2/k_1^* can be considered constant for the present purpose. Combining Eqs. (5), (9), and (10) leads to an expression for K_m :

$$K_m = Ce^{\Delta G_m/RT} + e^{\Delta G_d/RT}, \quad (11)$$

where C is a proportionality constant in which

$$C = k_2/k_1^*. \quad (12)$$

As pointed out below, the numerical value of K_m can be determined from Eq. (11); consequently, Eqs. (6) and (8) can be used to compare different sites in an RNA for antisense ODN hybridization. For this, we define a rate factor, $x = k/k_2$ such that from Eq. (6)

$$x = \frac{1}{Ce^{\Delta G_m/RT} + e^{\Delta G_d/RT}} \quad (13)$$

for steady-state reactions, and from Eq. (8)

$$x = \frac{1}{(Ce^{\Delta G_m/RT} + e^{\Delta G_d/RT}) + [S]} \quad (14)$$

for single-tube assays. x reflects the relative rate at which a specified site hybridizes with an antisense oligonucleotide. Eq. (13) is most useful for comparing relative hybridization rate at steady state, i.e. the components of a reaction are constantly generated and degraded such that their concentrations are constant. Steady-state reactions approximate intracellular conditions when cells grow exponentially (not to be confused with the stationary growth that would be achieved for a batch culture following exponential growth). Eq. (14) is most useful for estimation of initial hybridization rate (pre-equilibrium) in a single-tube assay.

The terms ΔG_m and ΔG_d can be readily determined from commercially available RNA folding programs (i.e. the GCG package, available from the University of Wisconsin) that estimate the energy changes associated with the formation of RNA secondary structures (Section 4). Our current estimates of the melting energy, ΔG_m , use the lowest free energy to determine the difference between target RNA folded without restriction (the pre-hybridization state, G_0 in Fig. 1) and target RNA folded with the region of hybridizing nucleotides restricted to a single-stranded condition (activated state, G_1 in Fig. 1). The value of k_2 , as well as that of C , are assumed to be similar for different sites in an RNA hybridizing to oligonucleotides when assayed by the same method under the same conditions. C can be estimated from the published data.

When antisense oligonucleotides are shorter than 15 nucleotides, we expect that the rate factor calculated using Eqs. (13) and (14) is proportional to the hybridization rate. For longer antisense oligonucleotides, hybridization begins with an initial contact between short regions of antisense and target RNA. The initial contact, called nucleation, is followed by rapid annealing. Maximal rate factor calculated for all possible 15-nucleotide regions in an antisense oligonucleotide is proposed to be proportional to nucleation rate.

2.2. Correlations between rate factor and experimental antisense-mRNA hybridization determined with oligonucleotide libraries

As a test for Eq. (14), we examined the relationship between the rate factor (x) and published values for hybridization of ODNs to sites in acetylcholinesterase mRNA [7]. In the experiment, mRNA was hybridized to a pool of 10-nucleotide-long random-sequence antisense ODNs. The oligonucleotides were allowed to bind mRNA in the presence of RNase H, and the

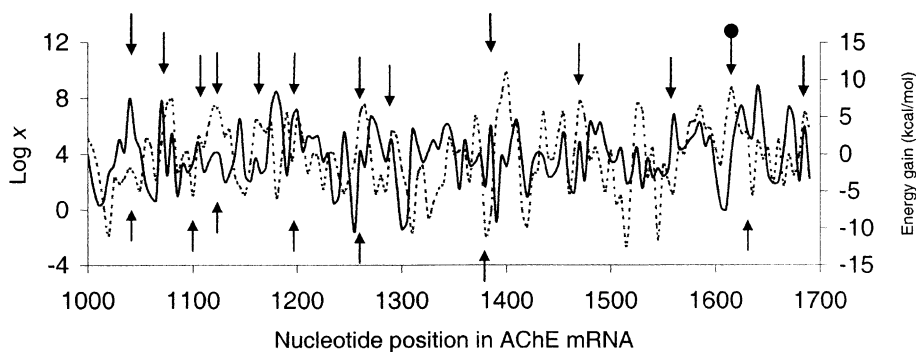


Fig. 2. Correlation between predicted and measured hybridization for antisense ODNs with acetylcholinesterase mRNA. Experimentally favorable sites for antisense hybridization (downward pointing arrows) were identified by gel electrophoresis following incubation with a random library of antisense oligonucleotides and treatment with RNase H. The data are taken from Fig. 3 of Birihk et al. [7] and cover a region of the mRNA from nucleotide positions 1000–1700. Calculated rate factors (x) for 10-nucleotide-long antisense DNAs (trace) were determined using Eq. (14) and plotted as a function of 5' positions of antisense binding sites in acetylcholinesterase mRNA. The arrow labeled \bullet indicates an experimentally favorable site predicted to be unfavorable. Upward pointing arrows below the trace indicate sites identified by the accessibility score method of Scherr et al. [4]. Calculated overall energy gain ($-\Delta G_{\text{overall}}$) using OligoWalk [9] is plotted as broken line.

most readily hybridized regions, which were degraded by RNase H, were then revealed by gel electrophoresis. By examining the published data, we identified favorable sites (downward pointing arrows, Fig. 2). We also calculated the rate factor (x) for all sites in the same region of acetylcholinesterase mRNA, five nucleotides apart (trace, Fig. 2). Most (12/13) of the arrows align with peaks in the trace. About half of the sites calculated to have $x > 10^4$ were identified experimentally as being favorable. Conversely, 85% of the favorable sites identified experimentally had a rate factor that was greater than 10^4 . Only one experimentally favorable site exhibited a low value of x .

2.3. Correlation between maximal rate factor and initial hybridization rate

For antisense oligonucleotides that are longer than 15 nucleotides, Eqs. (13) and (14) can be used to calculate a maximum rate factor by considering all possible 15-nucleotide regions within a given antisense oligonucleotide. If we assume that the 15-nucleotide region having the maximal rate factor corresponds to a nucleation site and if nucleation is rate limiting for hybridization, the maximal rate factor should reflect hybridization rate between the antisense nucleic acid and its target. We calculated maximal rate factors for hybridization of five antisense DNA oligonucleotides to an artificial 101-nucleotide RNA for which the second order binding reaction rate constant was derived from a mathematical formula for an experimentally determined hybrid-concentration time course [18]. The antisense DNAs, with lengths ranging from 17 to 37 nucleotides, were targeted to different sites as shown in Fig. 3(A) and Table 1. The maximal rate factor obtained for each antisense molecule (Table 1) showed a good correlation ($r = 0.95, p < 0.01$) with the second order binding reaction rate constant (Fig. 3(B)). A sixth oligonucleotide (HS2), which hybridized too slowly for measurement [18], had the lowest maximal rate factor (Table 1).

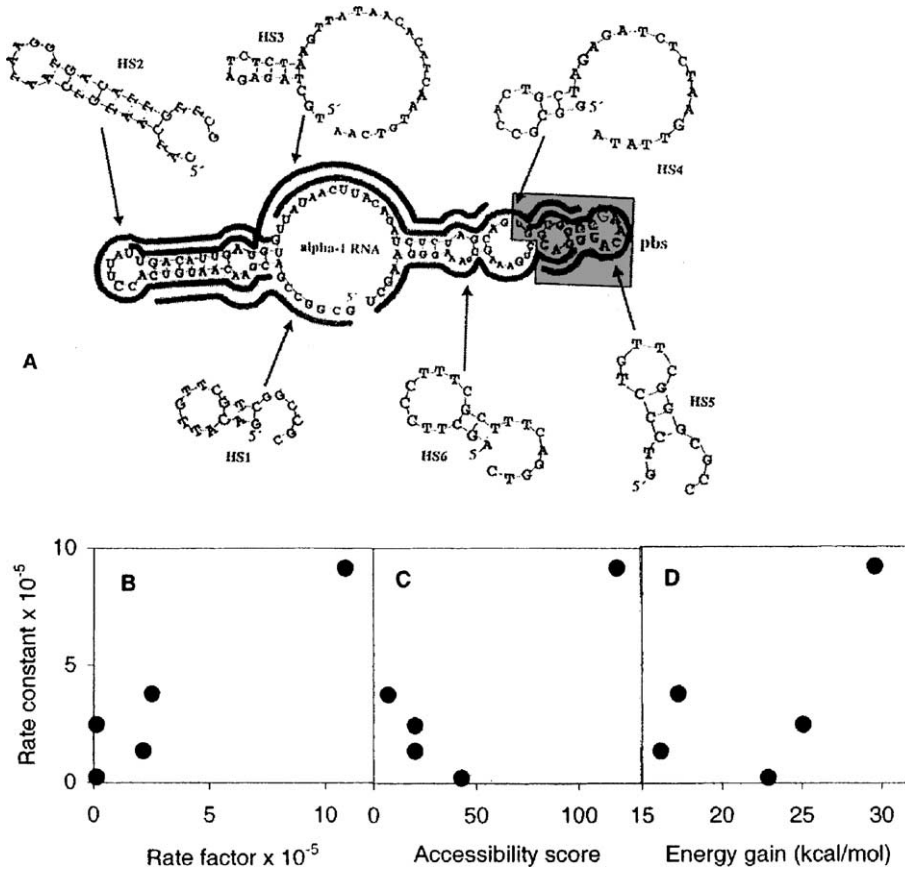


Fig. 3. Correlation between calculated rate factor and initial hybridization rate for short antisense DNA oligonucleotides interacting with an artificial RNA. (Panel A) Secondary structure of a 101-nucleotide RNA target, containing the replicative primer binding site of HIV-1. Also shown are six complementary antisense oligonucleotides. The panel is reproduced from Schwille et al. [18]. (Panel B) Correlation between calculated maximal value of rate factor and measured initial hybridization rate. Maximal values of rate factor (x in Eq. (14)) were determined for each antisense ODN shown in Panel A by first determining x for all sub-regions 15 nt long within each antisense oligo nucleotide (also in the RNA). Second order binding reaction rate constant of antisense DNA oligonucleotides to RNA was derived from a mathematical formula for hybrid concentration time course that was fitted to the experimental data by Schwille et al. [18]. (Panel C) Correlation between accessibility score by Scherr et al. [4] and binding reaction rate constant. (Panel D) Correlation between overall free energy gain by Mathews et al. [9] and binding reaction rate constant.

2.4. Hybridization predicted by single-strand analysis and by energy gain calculation

To identify accessible sites, Scherr et al. [4] proposed using an accessibility score that is based on a statistical consideration of single-strandedness. When the method is applied to acetylcholinesterase mRNA, it identifies seven sites as accessible (upward pointing arrows, Fig. 2). Experimentally, 13 were observed to be accessible (downward pointing arrows, Fig. 2). With one exception, the predicted sites coincided with observed sites. We also compared accessibility scores with experimental data for the six antisense oligonucleotides shown in Fig. 3(A). As originally

Table 1
Sequences of antisense ODNs for which hybridization rate to an artificial RNA have been measured

Name	Pairing region in RNA ^a	Sequence	Rate factor ^b	Acc. score ^c	Energy gain ^d (kcal/mol)	Measured rate constant ^e (1/M s)
HS1	1–19	GACATTGTTTCGTCGGCCGC	2.5×10^5	7	17.3	3.8×10^5
HS2	9–38	CATCAATGTCAATAAGGTGACATT-GTTCG	5.3	114	12.3	nd ^f
HS3	26–62	TGCTAGAGATCTCTAAGTTATAACA-CATCAATGTCAA	1.3×10^4	43	22.9	2.1×10^4
HS4	41–70	GGCGCCACTGCTAGAGATCTCTAA-GTTATA	1.3×10^4	20	25.1	2.5×10^5
HS5	65–81	GTCCCTGTTTCGGGCGCC	2.1×10^5	20	16.2	1.4×10^5
HS6	79–101	AGCTTCCCTTTCGCTTTCAGGTC	1.1×10^6	118	29.6	9.2×10^5

^a From Schwille et al. [18].

^b Calculated maximal rate factor using Eq. (14).

^c Calculated according to [4], but with an extension to include stretches as short as three nucleotides.

^d Calculated using OligoWalk of Mathews et al. [9].

^e Derived from experimentally determined mathematical relationship between hybrid concentration and time.

^f Not determined because the rate was too low.

described, the accessibility score model only assigns a score to motifs having a single-strand stretch longer than 10 nucleotides. By this criterion, only the site for antisense HS3 merits a score. However, we were able to obtain an accessibility score by extending the model to include shorter stretches (down to three nucleotides). An insignificant correlation between accessibility score and second order binding reaction rate constant was obtained (Fig. 3(C)).

We also examined the correlation between overall energy gain calculated by OligoWalk [9] and hybridization. When the OligoWalk calculation was applied to acetylcholinesterase mRNA, 9 of the 13 experimentally identified sites aligned with peaks in the profile (broken line, Fig. 2). As with the rate factor calculation, many calculated peaks were observed that were not found experimentally; in general, the peaks generated by the two calculations did not coincide (Fig. 2). For the hybridization experiment using the antisense oligonucleotides shown in Fig. 3(A), the correlation between second order binding reaction rate constant measured by Schwille et al. [18] and calculated overall energy gain by the OligoWalk method [9] was poor (see Fig. 3(D)).

3. Discussion

An expression was derived that relates nucleic acid secondary structure to the steady-state rate of oligonucleotide–RNA hybridization. The model is based on the assumption that hybridization of nucleic acids occurs through an intermediate state in which an initial short contact region has a single-stranded conformation prior to binding. This condition was approximated by using an RNA folding program that forces particular regions of RNA to be considered as single-stranded.

Two lines of evidence indicate that the rate factor expression (Eqs. (13) and (14)) can be used to help identify sites in an RNA target for hybridization with antisense oligonucleotides. First,

antisense–mRNA hybridization selected from random oligonucleotide libraries (Fig. 2) generally coincided with a high value of the calculated rate factor. Second, a good correlation was obtained between predicted and observed initial rates of hybridization for antisense deoxyribonucleic acids interacting with RNA (Fig. 3(B)).

The central feature of the rate factor model is that it uses both melting energy and energy gain to identify favorable sites for hybridization. Previous work has used either one or the other. The importance of using both factors is emphasized by comparison of the rate factor method with recent treatment of each factor alone [4,9]. When single-stranded regions, which presumably have low melting energy, are correlated with experimental hybridization, about half of the sites (6/13) in acetylcholinesterase mRNA were identified by calculation (upward pointing arrows, Fig. 2). For energy gain calculations [9], 9/13 of the experimentally identified hybridization sites corresponded to calculated peaks (broken line, Fig. 2). The rate factor method identified 12/13 sites with acetylcholinesterase mRNA (Fig. 2). Correlation of measured hybridization rate constant was insignificant with both the single-strand calculation and the overall energy gain method. With the rate factor method, the correlation was 0.95 ($p < 0.01$).

A direct consequence of using two energy parameters (melting energy and energy gain) for rate factor calculation is the prediction of a length optimum for antisense oligonucleotides when hybridizing to RNA: when length increases, ΔG_m increases and causes the rate factor in Eq. (13) to decline; at the same time, ΔG_d becomes more negative and causes the rate factor to increase. These opposing effects on rate factor create the optimal length effect. Models based on only one factor [2,4,8,9] do not explain the optimal length effect.

Not yet understood is why the rate factor calculation predicted many more sites to be accessible for hybridization than were actually observed using the oligonucleotide library method (Fig. 2). One explanation, which requires additional testing, is that the oligonucleotide library hybridization did not examine every site.

How well intracellular hybridization is modeled by the rate factor calculation has yet to be determined. Other work suggests that *in vitro* hybridization sometimes translates into inhibitory effects of antisense nucleic acids in living cells [19], and in one case an energy gain calculation correlated with inhibitory effects [9]. Since dynamic processes are more likely to be relevant than equilibrium processes for inhibition of gene expression with antisense oligonucleotides, the steady-state model should be more suitable than equilibrium models for identifying favorable hybridization sites. Additional tests are required to determine whether factors such as RNA tertiary structure and RNA-binding proteins occlude sites that would otherwise be predicted by calculation to be accessible for hybridization.

4. Materials and methods

4.1. Calculation of melting energy (ΔG_m) and energy difference (ΔG_d)

To determine the rate factor, x , for a given target site, the melting energy needed to form the hybrid and the energy gained upon formation of the hybrid were calculated from the free energy of the initial, the activated, and the final (hybridized) states (see Fig. 1). The initial free energies of the antisense and the target RNA ($G_{0 \text{ anti}}$ and $G_{0 \text{ target}}$) were obtained from the output files of the

GCG RNA folding program FoldRNA (GCG Package Version 10-Unix, Genetics Computer Group, University of Wisconsin, Madison, WI). The free energies for the activated antisense oligonucleotide ($G_{1 \text{ anti}}$) and the activated target RNA ($G_{1 \text{ target}}$) were approximated in the same way, but with the hybridization regions constrained in a single-stranded conformation, using the online command PREVENT. The free energy of hybridization, ΔG_h , was calculated using thermodynamic parameters measured by others [20]. We developed a program in C programming language for this calculation. This program is available upon request.

The energy of the final state, G_2 , the melting energy, ΔG_m , and the energy difference ΔG_d were calculated as follows:

$$G_2 = (G_{1 \text{ anti}} + G_{1 \text{ target}}) + \Delta G_h,$$

$$\Delta G_m = (G_{1 \text{ anti}} + G_{1 \text{ target}}) - (G_{0 \text{ anti}} + G_{0 \text{ target}}),$$

$$\Delta G_d = G_2 - (G_{0 \text{ anti}} + G_{0 \text{ target}}).$$

The values of ΔG_m and ΔG_d were then substituted into Eq. (13) or (14) to calculate rate factor. According to the definition, $C = k_2/k_1^*$, C may depend on assay conditions and on properties of the molecules involved in hybridization. A value of C can be estimated from several RNA–RNA hybridization measurements in the literature [21–23]; it varies from 10^{-6} to 10^{-8} . For the data shown in Fig. 3 we used $C = 10^{-7}$. For experiments involving RNase H, we have performed pilot ODN-mediated RNA cleavage and estimate $C = 10^{-11}$ by curve fitting. This value was used for Fig. 2. The variation of C with assay conditions and hybridization components is under investigation.

Acknowledgements

The work was supported by NIH Grants CA72860 and AI35257; P30 AI27742 (Center For AIDS Research, New York University Medical Center); and 2 P01 HL55435-06 and 5 P60 HL38655-13 (R. Nagel, P.I). We thank C. Benhan and F. Kramer for insightful discussion of the work.

References

- [1] V. Patzel, G. Sczakiel, In vitro selection supports the view of a kinetic control of antisense RNA-mediated inhibition of gene expression in mammalian cells, *Nucleic Acids Res.* 28 (2000) 2462.
- [2] R.E. Christofferson, J. McSwiggen, et al., Application of computational technologies to ribozyme biotechnology products, *J. Molecular Struct. (Theochem)* 311 (1994) 273.
- [3] V. Patzel, U. Steidl, et al., A theoretical approach to select effective antisense oligodeoxyribonucleotides at high statistical probability, *Nucleic Acids Res.* 27 (1999) 4328.
- [4] M. Scherr, J.J. Rossi, et al., RNA accessibility prediction: a theoretical approach is consistent with experimental studies in cell extracts, *Nucleic Acids Res.* 28 (2000) 2455.
- [5] L. Smith, K.B. Andersen, et al., Rational selection of antisense oligonucleotide sequences, *Eur. J. Pharm. Sci.* 11 (2000) 191.
- [6] Y. Ding, C.E. Lawrence, Statistical prediction of single-stranded regions in RNA secondary structure and application to predicting effective antisense target sites and beyond, *Nucleic Acids Res.* 29 (2001) 1034.

- [7] K.R. Birikh, Y.A. Berlin, et al., Probing accessible sites for ribozymes on human acetylcholinesterase RNA, *RNA* 3 (1997) 429.
- [8] R.A. Stull, L.A. Taylor, et al., Predicting antisense oligonucleotide inhibitory efficacy: a computational approach using histograms and thermodynamic indices, *Nucleic Acids Res.* 20 (1992) 3501.
- [9] D.H. Mathews, M.E. Burkard, et al., Predicting oligonucleotide affinity to nucleic acid target, *RNA* 5 (1999) 1458.
- [10] A. Jayaraman, S.P. Walton, et al., Rational selection and quantitative evaluation of antisense oligonucleotides, *Biochim. Biophys. Acta* 1520 (2001) 105.
- [11] M. Sohail, E.M. Southern, Selecting optimal antisense reagents, *Adv. Drug Deliv. Rev.* 44 (2000) 23.
- [12] S.P. Ho, D.H.O. Britton, et al., Potent antisense oligonucleotides to the human multidrug resistance-1 mRNA are rationally selected by mapping RNA-accessible sites with oligonucleotide libraries, *Nucleic Acids Res.* 24 (1996) 1901.
- [13] W.F. Lima, V. Brown-Driver, et al., Combinatorial screening and rational optimization for hybridization to folded hepatitis C virus RNA of oligonucleotides with biological antisense activity, *J. Biol. Chem.* 272 (1997) 626.
- [14] M. Sohail, H. Hochegger, et al., Antisense oligonucleotides selected by hybridisation to scanning arrays are effective reagents in vivo, *Nucleic Acids Res.* 29 (2001) 2041.
- [15] W.F. Lima, B.P. Monia, et al., Implication of RNA structure on antisense oligonucleotide hybridization kinetics, *Biochemistry* 31 (1992) 12055.
- [16] L. Pauling, The rate of chemical reactions, in: *General Chemistry*, Dover, New York, NY, 1988, p. 551 (Chapter 16).
- [17] L. Stryer, Introduction to enzymes, in: *Biochemistry*, W.H. Freeman, New York, 1990, p. 177 (Chapter 8).
- [18] P. Schwille, F. Oehlenschläger, et al., Quantitative hybridization kinetics of DNA probe to RNA in solution followed by diffusional fluorescence correlation analysis, *Biochemistry* 35 (1996) 10182.
- [19] O. Matveeva, B. Felden, et al., Prediction of antisense oligonucleotide efficiency by in vitro methods, *Nature Biotechnol.* 16 (1998) 1374.
- [20] N. Sugimoto, S.-I. Nakano, et al., Thermodynamic parameters to predict stability of RNA/DNA hybrid duplex, *Biochemistry* 34 (1995) 11211.
- [21] C. Persson, E.G.H. Wagner, et al., Control of replication of plasmid R1: kinetics of in vitro interaction between the antisense RNA, CopA, and its target, CopT, *EMBO J.* 7 (1988) 3279.
- [22] T.K. Stage-Zimmermann, O. Uhlenbeck, Hammerhead ribozyme kinetics, *RNA* 4 (1998) 875.
- [23] K.L. Schaefer, W.R. McClure, Antisense RNA control of gene expression in bacteriophage P22. II. Kinetic mechanism and cation specificity of the pairing reaction, *RNA* 3 (1997) 157.